



Iby and Aladar Fleischman
Faculty of Engineering
Tel Aviv University

הפקולטה להנדסה
ע"ש איבי ואלדר פליישמן
אוניברסיטת תל אביב

Project Report

2896

RF Oscillator and Wireless Transmitter

Students:

Mazz Shaikh 932056724
Nir Finch Cohen 230336612

Project carried out at: **Tel Aviv University**

For the project instructor:

I approve the submission of the following report

Edoh Shaulov

Contents

Contents

List of Figures

List of Tables

1	Introduction	2
1.1	Goals of the Project	2
1.2	Motivation	2
1.3	Approach	2
1.4	Existing Works and Potential Options	3
2	Theoretical Background	4
2.1	Oscillators	4
2.1.1	Introduction to Oscillators	4
2.1.2	Harmonic Oscillators: Feedback Oscillators	4
2.1.3	Colpits Oscillator	5
2.2	Matching Networks	5
2.2.1	T Matching Network	6
2.3	Antennas	7
2.3.1	Microstrip Patch Antenna	7
2.3.2	Wideband Patch Antenna	8
3	Implementation	10
3.1	BFP520/INF - Transistor Choice	10
3.2	Matching Network	10
3.3	Oscillator System	11
3.4	Antenna	12
3.5	Components	12
3.6	PCB Layout	13
4	Simulations	14
4.1	Matching Network	14
4.2	Oscillator	14
4.2.1	Transient Simulation	14
4.2.2	Harmonic Balance Simulation	16
4.3	Antenna	16
4.4	S-parameter (S11) Simulation	16
4.5	Far Field Simulation	17
5	Analysis of Results	18
5.1	Matching Network	18
5.2	Oscillator	18
5.2.1	Transient Simulation	18
5.2.2	Harmonic Balance Simulation	18
5.2.3	Efficiency of Oscillator	18
5.3	Antenna	19
5.3.1	S-parameter (S11) Simulation	19
5.3.2	Far Field Simulation	19
5.4	Testing in Lab	19
5.4.1	Adding Ground to the PCB board	19
5.4.2	Testing the extended Circuit	20
5.4.3	Obtained Spectrum	20

6 Conclusion and Further Work	21
7 Project Documentation	22
8 Appendix	23
8.1 BFP520 Data	23
8.2 Matching Network	23
8.2.1 Computation of L_s and C_s	23
8.3 Oscillator	24
8.3.1 Mathematical Model of Feedback Oscillators	24
8.3.2 Operating Frequency and Startup Condition for Colpits Oscillator	25
8.4 Transmission Line Formulas	26
8.4.1 Parameters of a Microstrip line for required Z_0	26
8.4.2 Patch Antenna Dimensions	27
8.4.3 Constraints on the dimensions of the ground plane	27
8.5 Antenna	28
8.5.1 Far-Field Simulation Output	28
8.6 Layout	28
8.6.1 Table of Components	28
8.6.2 PCB Schematic	29
References	30

List of Figures

1 Two common LC oscillator circuits, the Hartley and Colpitts oscillators	4
2 Colpitts oscillator	5
3 T-Matching Network	6
4 Microstrip Patch Antenna with Inline Feed	7
5 Wideband Patch Antenna	8
6 Transient Analysis	9
7 Oscillator+Matching Network Topology	11
8 Layout	13
9 Matching Network S-parameters	14
10 Transient Analysis	15
11 Harmonic of Oscillator+Matching Network	16
12 S11 of Wideband Patch Antenna	17
13 (a) Ground Connection to the PCB, and (b) Complete Test Setup	20
14 Spectrum Analyzer connected to the receiver	20
15 Combined plots of the BFP520's key characteristics.	23
16 Block diagram of a feedback linear oscillator	24
17 Small Signal Model for Colpits Oscillator	25
18 Far-Field of Wideband Patch Antenna	28
19 Oscillator+Matching Network Schematic	29

List of Tables

1 Output from Python Script for Matching Network	11
2 Antenna Measurements from Python	12
3 Far-Field Characteristics	17
4 Used Components and Tolerances	28

List of Equations

2 Resonator Length in Wideband Patch Antenna	8
--	---

6	T-Matching Network Source Components	24
7	T-Matching Network Load Components	24
10	Barkhausen Criteria 1	25
11	Barkhausen Criteria 2	25
13	Small Signal Analysis of Oscillator	25
14	Oscillator Operating Frequency	26
16	Startup Condition on R_L	26
17	Characteristic Impedance of Microstrip Line	26
19	Solution of W for a microstrip line for $W/d < 2$	26
20	Solution of W for a microstrip line for $W/d > 2$	26
22	Width of Patch Antenna	27
23	ϵ_{eff} of Patch Antenna	27
24	Excess Length (ΔL) of Patch Antenna	27
25	Effective Length of Patch Antenna	27
27	Ground Plane constraints for proper functioning of Patch Antenna	27

Abstract

In the rapidly evolving field of wireless communication, the development of efficient and reliable antennas that operate at high frequencies is crucial. This project focuses on the design and implementation of a high-frequency oscillator tuned to approximately 3.5 GHz, intended for integration into a sophisticated antenna system. The primary objective is to enhance the functionality of the transmitter antenna by interfacing the oscillator with a carefully designed matching network, thereby aiming to achieve superior performance benchmarks in communication systems.

The project encompasses several key disciplines including Radio Frequency (RF) engineering, Microwave engineering, and Analog Integrated Circuits. Designing RF systems that operate effectively at frequencies around 3.5 GHz requires a deep understanding of circuit theory, analog circuits, frequency response, electromagnetic principles, and communication systems. By combining these domains, the project seeks to advance the state-of-the-art in wireless communication technology.

Oscillators are fundamental components in many applications due to their ability to generate stable and precise periodic waveforms. The high-frequency oscillator developed in this project is expected to have significant applications in areas such as 5G networks, satellite communication systems, radar technologies for navigation, RFID tags used in smartcards, and Magnetic Resonance Imaging (MRI). This highlights the extensive impact that a well-designed oscillator can have across various industries, beyond just antenna systems.

The project follows a structured implementation plan, beginning with the development of an oscillator model. This model is validated through Spice simulations to ensure its effectiveness at the targeted frequency of 3.5 GHz. The next phase involves selecting suitable components, including the optimal transistor—whether an NPN BJT or an NMOS transistor—to operate within the designated frequency range. This selection process includes creating and validating a corresponding spice model and simulating it using Cadence Virtuoso to evaluate S-parameters.

Integration of the oscillator with the transmitter antenna requires careful attention to antenna matching. This process is essential for optimizing power transfer and minimizing signal reflections. The project emphasizes the importance of this integration, which is facilitated by the matching network, to ensure good operation within the broader communication ecosystem. Additionally, a compact and optimized Printed Circuit Board (PCB) layout will be designed to reduce parasitic elements and signal loss, crucial considerations in RF design.

The final phase of the project involves a rigorous testing regimen to validate the oscillator's performance. Using a pre-built receiver, the oscillator's stability, frequency accuracy, and signal fidelity will be thoroughly assessed. This comprehensive testing is critical to confirm the oscillator's readiness for real-world communication systems and to ensure it meets the required performance standards.

In summary, this project provides an in-depth exploration of designing and implementing a high-performance 3.5 GHz oscillator. By combining theoretical insights, simulation-based validation, and practical testing, the project aims to advance antenna systems and contribute to improvements in efficiency, precision, and reliability across a range of technological applications.

1 Introduction

1.1 Goals of the Project

The primary objective of this project was to comprehensively design, simulate, and test a 3.5GHz Colpitts RF oscillator, accompanied by a fabricated matching network and antenna, to demonstrate the practical and theoretical underpinnings of RF communication systems. The overarching goal was to develop an oscillator that not only functions efficiently at the specified frequency but also exhibits high stability, low phase noise, and an output power level conducive to real-world applications in RF communication systems, particularly those relevant to modern 5G networks. While the circuit designed in this project is not a complete transmitter, the intent is to offer a cohesive simulation and analysis of three critical hardware components essential to RF communication systems. Through this project, we aim to gain substantial exposure to RF design principles, as well as electromagnetic (EM) and printed circuit board (PCB) design techniques. Specifically, our goal was to design a 3.5GHz oscillator, integrate it with a matched microstrip antenna, fabricate the design on a PCB, and rigorously test it within the RFIC Lab at Tel Aviv University (TAU).

1.2 Motivation

The rapid evolution and expansion of wireless communication technologies, particularly marked by the recent deployment of 5G networks, have significantly heightened the demand for RF frequency oscillators that can deliver stable, precise signals. The 3.5GHz frequency band, a critical component of the C-band spectrum, is especially vital for 5G due to its optimal balance between signal range and available bandwidth, making it a focal point for many 5G deployments.

This project focuses on the Colpitts oscillator, a time-tested and widely used topology in RF circuits, selected for its robustness and reliability in generating high-quality signals with minimal distortion. The design includes a customized matching network to optimize space and ensure precise frequency alignment with the antenna, which is crucial for maximizing the oscillator's efficiency and overcoming the limitations of off-the-shelf components. By enhancing stability and boosting power efficiency, this tailored oscillator design not only meets the stringent demands of modern 5G networks but also achieves cost efficiency by streamlining the design process without compromising performance.

Through this project, we aim to contribute to the advancement of RF design, addressing the growing need for precise frequency control and stability in the context of emerging 5G technologies.

1.3 Approach

To accomplish the project's objectives, a structured and meticulous approach was adopted. The design process commenced with an in-depth theoretical analysis of the Colpitts oscillator, focusing on critical design parameters such as transistor selection, biasing conditions, and feedback network configuration. The small signal model of the oscillator was carefully analyzed, with its characteristics justified through rigorous reasoning, as will be elaborated in subsequent sections. Following the theoretical groundwork, the oscillator was simulated using advanced tools like SPICE and Virtuoso, enabling us to model its behavior under various operational conditions and component choices. These simulations were crucial in ensuring that the design met the stringent performance criteria required for 3.5GHz operation.

Upon successful simulation, the next phase involved the design of a matching network. This network was engineered to optimize impedance matching between the oscillator and the antenna, thereby minimizing reflection losses and maximizing power transfer.

The antenna design, executed using CST software, was specifically tailored to operate efficiently at 3.5GHz, ensuring that the entire system was well-integrated and capable of delivering optimal performance. The final phase of the project involved testing the complete circuit.

1.4 Existing Works and Potential Options

In the course of the project, the Colpitts oscillator was evaluated against other commonly employed oscillator designs, such as the Hartley oscillator and the ring oscillator, to assess its suitability for the 3.5GHz frequency range and to determine which topologies might offer the most promising alternatives. The Hartley oscillator, characterized by its use of an inductive divider within its tank circuit, is often favored for its simplicity and ease of tuning. However, at RF frequencies like 3.5GHz, the Colpitts oscillator, with its capacitive divider, offers superior frequency stability and reduced phase noise, making it a more reliable and practical choice for RF communications. The Colpitts topology is also more frequently employed in practice, further supporting its selection for this project. On the other hand, the ring oscillator, which operates by utilizing a series of phase-inverting stages connected in a feedback loop, is known for its simplicity and ease of integration into digital circuits. Despite these advantages, ring oscillators typically suffer from higher phase noise and less frequency stability, rendering them less suitable for high-performance RF applications where precise frequency control is paramount. After careful consideration of these factors, the Colpitts topology emerged as the most appropriate choice for this project, offering a compelling balance of performance, stability, and practicality for 3.5GHz RF communication systems.

2 Theoretical Background

2.1 Oscillators

2.1.1 Introduction to Oscillators

Oscillators are fundamental components in a wide range of electronic systems, providing periodic waveforms necessary for various applications, including signal generation, timing, and frequency control. The importance of oscillators spans multiple domains, from communications and instrumentation to consumer electronics and industrial systems. Their ability to generate stable and precise frequencies makes them indispensable in both analog and digital circuits.

At their core, oscillators convert a direct current (DC) input into an alternating current (AC) output, producing a waveform that can be sinusoidal, square, triangular, or sawtooth, depending on the design and application requirements. The basic principle behind oscillation involves positive feedback, where a portion of the output signal is fed back to the input in phase with the original signal, thereby sustaining the oscillation.

There are several types of oscillators, each tailored to specific applications and performance criteria. Common categories include harmonic oscillators, which generate sinusoidal outputs, and relaxation oscillators, which produce non-sinusoidal waveforms. Examples of harmonic oscillators are the Colpitts, Hartley, and Clapp oscillators, while relaxation oscillators include the astable multivibrator and the Schmitt trigger oscillator.

In this project, we focus on Harmonic Feedback Oscillators.

2.1.2 Harmonic Oscillators: Feedback Oscillators

Harmonic oscillators, or feedback oscillators, generate sinusoidal outputs and are widely used for their ability to produce stable and precise frequencies. These oscillators rely on positive feedback, where a portion of the output signal is fed back to the input in phase, sustaining oscillation. Common types include the Colpitts, Hartley, and Clapp oscillators.

The feedback network typically consists of inductors and capacitors forming an LC tank circuit. The choice of components and the design of the feedback network determine the oscillation frequency. Harmonic oscillators are preferred in RF applications due to their low phase noise and high frequency stability, making them ideal for communication systems and frequency synthesizers.

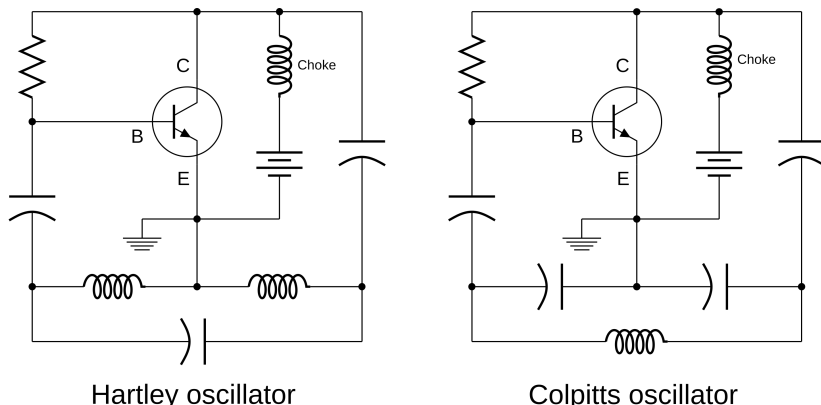


Figure 1: Two common LC oscillator circuits, the Hartley and Colpitts oscillators

2.1.3 Colpitts Oscillator

The Colpitts oscillator is a popular LC oscillator known for generating stable, high-frequency sinusoidal signals. It is particularly advantageous for frequencies around 3.5[GHz] due to its reliable performance and simplicity in design. [6]

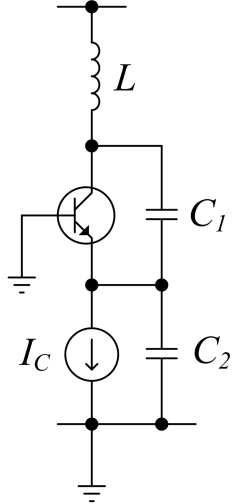


Figure 2: Colpitts oscillator

2.1.3.1 Working Principle of Colpitts Oscillator

The Colpitts oscillator operates based on the principle of positive feedback, where a portion of the output signal is fed back to the input in phase, sustaining continuous oscillation. The basic configuration of a Colpitts oscillator includes an active component, such as a transistor or an operational amplifier, and a feedback network comprising two capacitors and an inductor (*LC* tank circuit).

The essential elements of a Colpitts oscillator can be summarized as follows:

- **Active Device:** This can be a transistor (BJT or FET) or an operational amplifier, which amplifies the signal and provides the necessary gain for oscillation.
- **LC Tank Circuit:** The feedback network consists of two capacitors (C_1 and C_2) connected in series and an inductor (L) connected in parallel with the capacitor combination. The point where the capacitors are joined is connected to the input of the active device, while the other ends are connected to the output and ground.
- **Feedback Mechanism:** The voltage across C_2 is applied to the base-emitter junction of the transistor, as feedback to create oscillations

The frequency of oscillation is primarily determined by the values of the capacitors (C_1 and C_2) and the inductor (L), given by $\omega_0 = \sqrt{\frac{1}{L \frac{C_1 \cdot C_2}{C_1 + C_2}}}$. For sustained oscillations, we need $-(-r_\pi CL_p R_L g_m + 2r_\pi CL_p + CL_p R_L)\omega_0^2 + R_L > 0$ ¹

2.2 Matching Networks

Matching networks are essential components in RF (Radio Frequency) and microwave engineering, designed to match the impedance between a source and a load. Impedance matching is

¹Startup condition solved for case $C_1 = C_2 = C$. Proof in Appendix

crucial to maximize power transfer and minimize reflections in a circuit. When the impedances are not matched, power is reflected toward the source, which can lead to inefficiencies, signal loss, and potential damage to components. Matching networks can be composed of various types of components, including resistors, capacitors, inductors, and transformers. The choice of components and the network topology depends on the specific requirements of the application, such as the frequency range, bandwidth, and power handling capabilities. Common types of matching networks include:

- **L Networks:**
 - Consists of a series and a parallel component (either inductors or capacitors).
 - Simple and suitable for narrowband applications.
- **T Networks:**
 - Consists of two series components and one parallel component.
 - Versatile and can provide better matching over a broader range of frequencies.
- **Π Networks:**
 - Similar to T networks but with two parallel components and one series component.
 - Often used in high-power applications and for impedance transformation over a wide range.

2.2.1 T Matching Network

A T-matching network consists of inductors and capacitors arranged in a T-shaped topology. The primary purpose is to match the impedance between a source and a load to ensure maximum power transfer and minimal reflection. In a T-matching network, we have²

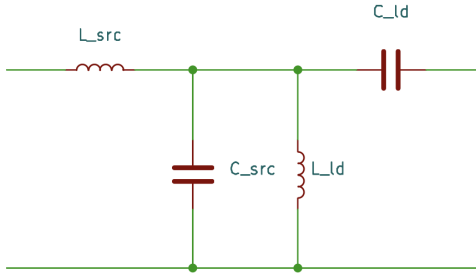


Figure 3: T-Matching Network

- L_{src} (Source Inductance): The inductance component connected in series with the source.
- C_{src} (Source Capacitance): The capacitance component connected in parallel with the source.
- L_{ld} (Load Inductance): The inductance component connected in series with the load.
- C_{ld} (Load Capacitance): The capacitance component connected in parallel with the load.

²Computation algorithm can be found in Appendix

2.3 Antennas

2.3.1 Microstrip Patch Antenna

A microstrip patch antenna is a type of radio antenna that consists of a flat rectangular sheet or "patch" of metal, mounted over a larger sheet of metal called a ground plane. The patch and the ground plane are separated by a dielectric substrate. These antennas are widely used in various wireless communication systems, including those integrated into integrated circuits (ICs) and printed circuit boards (PCBs).



Figure 4: Microstrip Patch Antenna with Inline Feed

Microstrip Patch Antenna Components:

- **Patch:** Conductive layer (typically copper) serving as the radiating element.
- **Ground Plane:** Larger conductive layer providing a reference plane.
- **Dielectric Substrate:** Insulating material between the patch and ground plane, influencing resonant frequency and bandwidth.

Design Considerations:³

- **Patch Shapes:** Rectangular is most common for easy analysis and fabrication; circular and triangular shapes are also viable.
- **Operation:** Radiates electromagnetic waves from edges when excited by RF signals; electric field forms between patch and ground plane.
- **Integration with IC/PCB:**
 - **Compact Size:** Fits in space-limited applications, ideal for ICs and PCBs.
 - **Low Profile:** Thin design integrates seamlessly with surfaces.
 - **Cost-Effective:** Standard PCB fabrication keeps production costs low.
- **Frequency Versatility:** Adjustable patch dimensions and substrate properties allow operation across various frequencies.

³Detailed Mathematical formulations can be found in Appendix

2.3.2 Wideband Patch Antenna

2.3.2.1 Reason for Usage

Microstrip patch antennas generally have a narrow bandwidth [1]. This makes them less suitable for wideband applications. To handle fabrication variations in the oscillating frequency of the oscillator, a different topology consisting of coupled resonators was used [7]. Coupled resonators provide a viable solution for enhancing the bandwidth of microstrip patch antennas. By introducing additional resonant structures in proximity to the primary patch, significant improvements in bandwidth can be achieved without compromising other essential antenna characteristics. This technique is highly effective for wideband wireless communication systems, offering a practical approach to overcoming the limitations of narrow bandwidth in microstrip patch antennas.

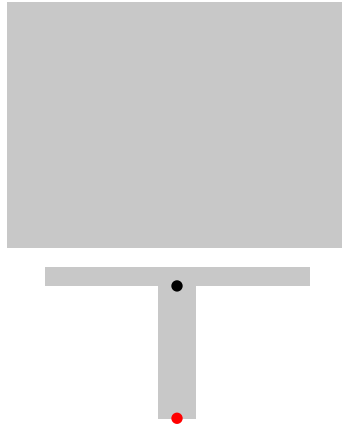


Figure 5: Wideband Patch Antenna

2.3.2.2 Basic Working Principle

Coupled resonators are additional patches or slots that are positioned in proximity to the primary patch antenna. These resonators are designed to have resonant frequencies close to the primary patch's resonant frequency. The interaction between the primary patch and the coupled resonators leads to the formation of multiple resonant modes, effectively broadening the overall bandwidth. The dimensions of path and the resonators can be computed using (8.4.2)

2.3.2.3 Design Method

Due to the compact and symmetrical geometry of the proposed antenna, there are only a few parameters that need to be determined in our antenna design. The design process involves determining the sizes of the patch ($L_p \times W_p$) and the $\lambda/4$ resonators ($L_r \times W_r$) based on the specified central frequency f_0 . The resonant frequencies of the patch and the $\lambda/4$ resonators primarily depend on their lengths, L_p and L_r , respectively. This can be estimated by considering the influence of the coupling gap d on the reflection coefficient, as illustrated in (5).

$$L_p = \frac{1}{2f\sqrt{\epsilon_{rp}}\sqrt{\mu_0\epsilon_0}} - 2\Delta L \quad (1)$$

$$L_r = \frac{1}{f\sqrt{\epsilon_{rr}}\sqrt{\mu_0\epsilon_0}} \quad (2)$$

where ΔL is the effective extended length because of the parasitic effects at the two edges of a rectangular patch and ϵ_{ri} can be found using (23).

Due to the compact and symmetrical geometry of the proposed antenna, there are only a few parameters that need to be determined in our antenna design. The design process involves determining the sizes of the patch ($L_p \times W_p$) and the $\lambda/4$ resonators ($L_r \times W_r$) based on the specified central frequency f_0 . The resonant frequencies of the patch and the $\lambda/4$ resonators primarily depend on their lengths, L_p and L_r , respectively. This can be estimated by considering the influence of the coupling gap d on the reflection coefficient, as illustrated in (5). The second step is to determine the width d of the gap. Because of the emergence of two resonances introduced by the patch and the paired $\lambda/4$ resonators, two reflection poles can be expected to appear in the reflection coefficient. These two poles can be appropriately adjusted by the gap width d , aiming to realize a dual-pole wideband performance.

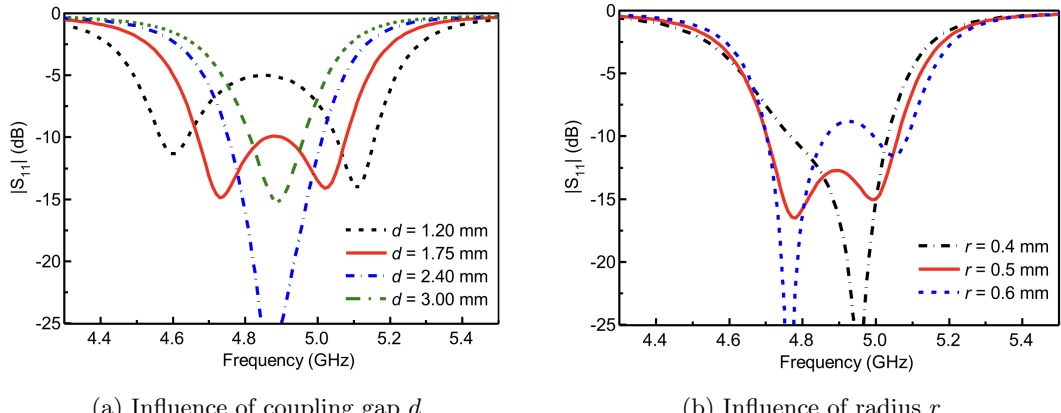


Figure 6: Transient Analysis

Fig. 6a⁴ displays the variation of reflection coefficients with respect to d . As the two resonators are closely placed with $d = 1.2$ mm, two reflection poles can be observed in Fig. 6a. However, they are far away from each other, which can be applied to design a dual-frequency antenna. With the increase in d , the two poles gradually close up and are finally combined together to create a wide operating band when $d = 1.75$ mm. In this case, the bandwidth reaches its maximum, which is nearly three times wider than that of a traditional patch antenna formed on the same substrate. If d is further increased, the two poles are merged into a single pole at $d = 2.4$ mm, and then poor impedance matching happens at $d = 3$ mm or more. Against the traditional insert-fed patch antenna, the proposed patch antenna can achieve adjustable bandwidth as illustrated in Fig. 6a.

Generally speaking, acceptable performance can be obtained after the above two steps are executed. The shorting pin in the feeding structure is a portion of the paired $\lambda/4$ resonators and its radius r can be chosen arbitrarily. Fig. 6b displays the variation of the simulated reflection coefficients with respect to pin radius r . We can figure out that the pin radius has little influence on the reflection coefficient herein.

In addition to bandwidth enhancement as described above, the undesired harmonic radiation at high frequencies can be effectively suppressed by the proposed technique

⁴Plots taken from [7]

3 Implementation

3.1 BFP520/INF - Transistor Choice

The BFP520 from Infineon is an excellent choice for designing an oscillator at 3.5 GHz due to its high-frequency performance, low noise figure, and high gain. Below, we discuss the specific features that make the BFP520 suitable for this application, supported by relevant data from its datasheet.⁵

- **High-Frequency Performance:** The BFP520 is optimized for frequencies up to 10 GHz, with a transition frequency (f_t) of approximately 50 GHz. This high f_t ensures efficient operation at 3.5 GHz, providing the necessary amplification for stable oscillation.
- **Low Noise Figure:** The noise figure is critical for oscillator performance, as it affects phase noise. The BFP520 has a low noise figure of around 1.4 dB at 3.5 GHz, which is essential for maintaining signal clarity and integrity in communication systems.
- **High Gain:** The transistor provides a high gain of approximately 16 dB at 3.5 GHz, which helps overcome circuit losses and ensures a strong and stable output signal.

Using the BFP520 for a 3.5 GHz oscillator ensures high performance due to its excellent high-frequency capabilities, low noise figure, and high gain. These features make it an ideal choice for stable and efficient oscillator design in RF applications.

3.2 Matching Network

Calculations for the matching networks were performed using Python. The objective was to design a T-topology matching network to match the antenna impedance to a high impedance for high voltage swing. In this case, the source and the load impedances are defined as follows:

- **Source Impedance:** This is the antenna impedance
- **Load Impedance:** This is the impedance we want the oscillator to see as it's load

The feedline of the antenna will be designed to have an impedance of $50[\Omega]$. This impedance was to be matched to a high value in order to get high swings on the antenna's feedline. The target impedance was simulated by connecting it directly to the oscillator in Virtuoso Spectre so as to check the magnitude of the voltage swings. The following 2 tradeoff were taken into consideration:

1. Large value seen by the oscillator at it's operating frequency to get large swings
2. Small enough so that along with large swing, a large bandwidth⁶ can be maintained

The value of $10^3[\Omega]$ was chosen to have a good balance between the high magnitude of impedance seen by the oscillator, and to have large bandwidth where the impedance remains high, preferably staying at 90% of it's value in the interval of $3.4[Ghz] \rightarrow 3.7[Ghz]$. This was done so to avoid loss of efficiency due to slight changes in the operating frequency due to manufacturing defects.

The reactance values obtained from Python can be seen in Table(1)

⁵Data given by Infenion. Can be found in Appendix

⁶The bandwidth is the range of frequencies where a large enough impedance is seen (what impedance is large enough was determined through Spectre sweeps)

Variable	Value	Variable	Value
f_0	3.5×10^9	C_{src}	2.02955×10^{-15}
Z_{out_osc}	1000	Q_{ld}	4.36348
Z_{load}	50	$X_{parallel_ld}$	229.633
Z_{center}	1002	X_{series_ld}	218.174
Q_{src}	0.0447214	L_{ld}	1.04421×10^{-8}
$X_{parallel_src}$	22405.4	C_{ld}	2.08424×10^{-13}
X_{series_src}	44.7214	C_{com}	2.10454×10^{-13}
L_{src}	2.03361×10^{-9}	L_{com}	1.70212×10^{-9}

(a) Source Variables

(b) Load Variables

Table 1: Output from Python Script for Matching Network

3.3 Oscillator System

We used the formulas from the theoretical section of the report to set the operating point and startup conditions of the oscillator. These calculations were essential for guiding our design and ensuring that everything would work as intended.

To get the oscillator to hit the exact frequency we needed, a series of sweeps were run using Virtuoso Spectre, allowing us to tweak and fine-tune the circuit components until to achieve the precise frequency.

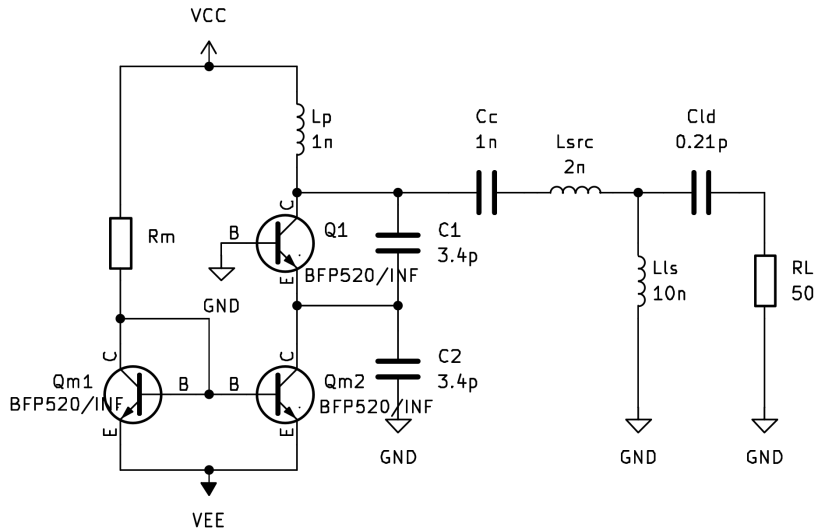


Figure 7: Oscillator+Matching Network Topology

An important part of our setup was the matching network, which we used to connect the oscillator to the load. This network plays a crucial role in making sure the impedance is matched properly, which helps to minimize reflections and maximize power transfer. We spent some time selecting and optimizing the components of the matching network to get the best performance. The capacitor of $2[pF]$ obtained in Table 1 was removed as it had very little influence on functioning of the network due to its large value and open behaviour at operating frequencies.

Overall, the process was a blend of theory and hands-on adjustments. By applying the theoretical principles and fine-tuning through simulations, we managed to build a reliable oscillator that meets our design goals.

3.4 Antenna

We first used Python to measure the antenna dimensions, writing scripts to analyze the design parameters and determine the precise measurements needed⁷

Table 2: Antenna Measurements from Python

Parameter	Value [mm]
H	1.52
W	28.08
L	21.69
y_0	7.89
W_{gnd}	51.65
L_{gnd}	45.26
W_{feed}	4.70

We chose a Rogers substrate due to its low loss and stable dielectric properties, which are ideal for high-frequency applications. The substrate's high dielectric constant and low dissipation factor were key for minimizing signal loss and ensuring efficient transmission at 3.5 GHz.

The antenna model was then created in CST (Computer Simulation Technology) and fine-tuned. We ran simulations for two key parameters:

- **S-Parameter:** The S_{11} parameter measures how much signal is reflected back due to impedance mismatch, indicating the efficiency of the antenna. A low S_{11} value signifies effective signal transmission.
- **Far-Field:** The far-field radiation pattern shows how the antenna radiates energy into space, which is important for assessing directivity, gain, and overall performance.

Simulating both S_{11} and far-field patterns gave a complete view of the antenna's performance, covering both impedance matching and radiation characteristics.

3.5 Components

The components were sourced from JLCPCB. In order to make proper choice for components, the following analysis was done using datasheets and simulations⁸

1. Identification of components in the system which require low tolerances and are critical to performance, done using circuit understanding and simulations
2. Identification of component values available to source, followed by rounding the said values in Spectre to identify possible small changes in the operations
3. Identification of the maximum permissible tolerances by sweeping component values in Spectre and choosing components which satisfy the tolerance constraints
4. Making minor changes in circuit topology to cater it to available component values

After performing the above analysis, we arrived at a set of components that may be viewed in Table - in the Appendix

⁷All the measurements are in accordance with JLCPCB guidelines - <https://jlcpcb.com/capabilities/pcb-capabilities>

⁸Complete component list can be found in Appendix

3.6 PCB Layout

The PCB layout design was completed using Altium designer. Initially, the project was opened and the schematic, describing only the theoretical component connections, was drawn on the Altium interface. Precise components that fulfilled the simulated requirements were chosen and placed on the schematic, which can be viewed in Appendix - Figure 18.

When choosing components, we had to be assiduous regarding the tolerance of the components. For instance, in practice, we opted to form the tank using two $2[nH]$ inductors connected in parallel as opposed to one $1[nH]$. This was because the lowest available tolerance for these components was in the region of $0.1[nH]$, which, after simulating, in its extreme, was found to knock the output frequency out of the feedband of the antenna. However, opting for two inductors of the same tolerance in parallel, reduced the error by 50% in the following way.

$$Z_{\text{tot}} = (L + \epsilon)j\omega \parallel (L + \epsilon)j\omega = \frac{1}{\frac{1}{L+\epsilon} + \frac{1}{L+\epsilon}} = \frac{L}{2} + \frac{\epsilon}{2}$$

We can see that taking $L = 2[nH]$ yields an equivalent $1[nH]$ inductance with half the error.

In addition, we also had to construct the model of the antenna using the data taken from the CST simulation. This had to be implemented as a two input device. The dimensions of the device were written into the physical model.

After assembling the schematic and routing upon it, the physical PCB routing needed to be completed. This was done with ease due to the pre-routing feature on the Altium software. We adhered standard protocols for routing RF PCBs such as 45 degree turns in the trace as opposed to 90, in order to reduce parasitic capacitances that are likely to result in RF shorts at trace junctions. In addition, we saw that the easiest implementation of the current mirror came with rotating one of the transistors by another 90 degree, deviating from the schematic plan so as to have optimal routing. Once finished, the PCB layering was organised with specific vias connecting between the bottom ground plane and the relevant component nodes.

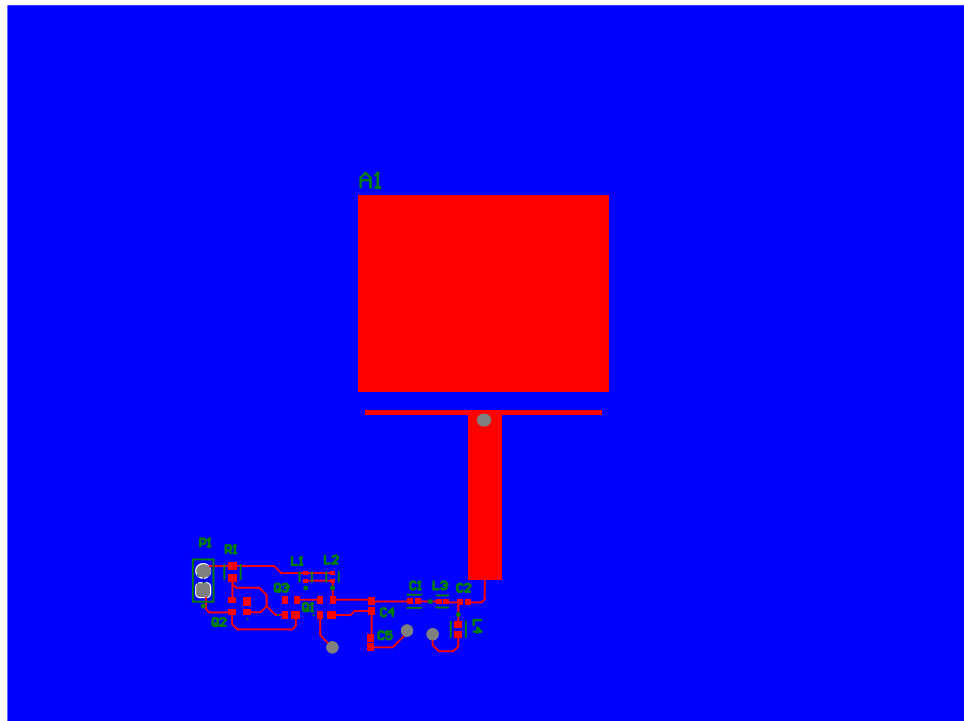


Figure 8: Layout

4 Simulations

Simulations were conducted using the following software tools:

- **Oscillator:** The initial design and working prototype were developed using PSpice. Final component parameters and worst-case scenario analyses were performed with Cadence Virtuoso (Spectre simulations).
- **Matching Network:** Calculations were executed using Python, while simulations were carried out using .ac analysis in LTSpice.
- **Microstrip Patch Antenna:** Calculations were conducted using Python, with simulations and parameter finalization performed in CST Suite.

4.1 Matching Network

The circuit (3) was analyzed as a 2-port system using S-parameters

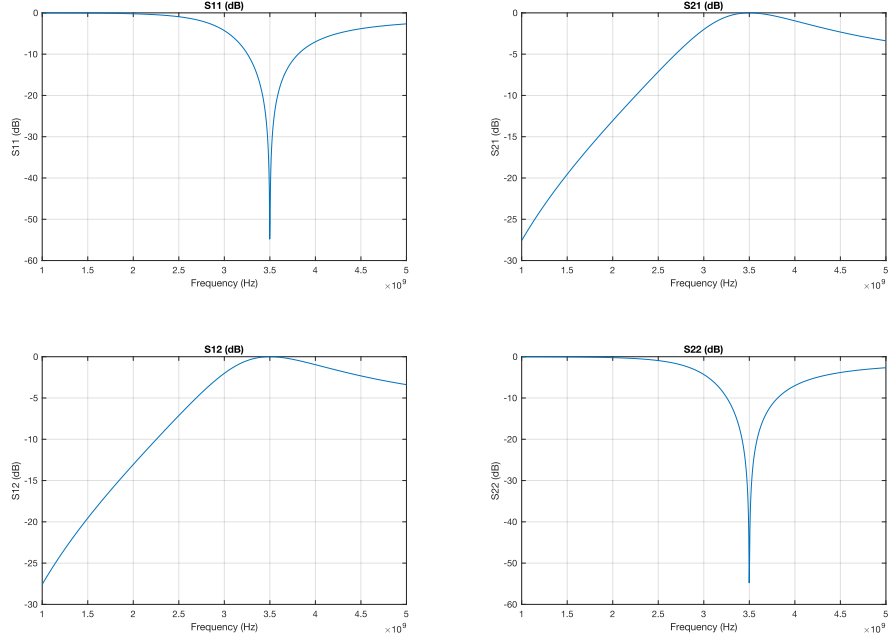


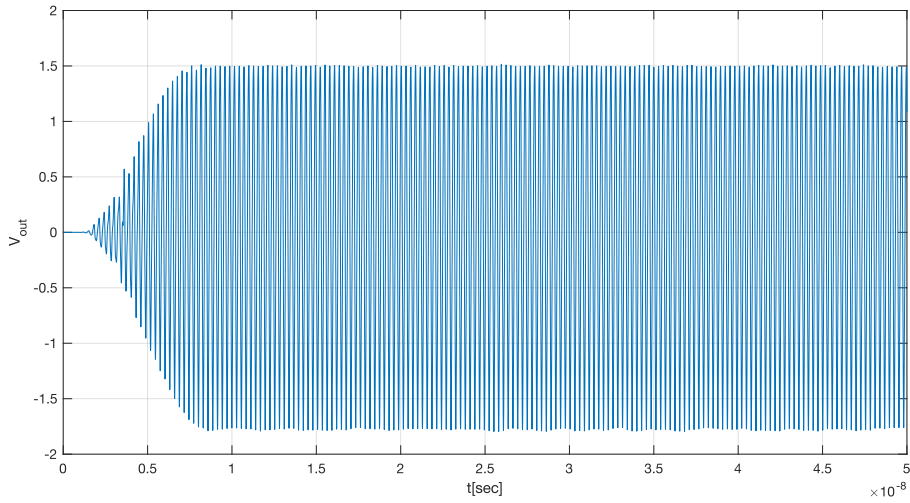
Figure 9: Matching Network S-parameters

4.2 Oscillator

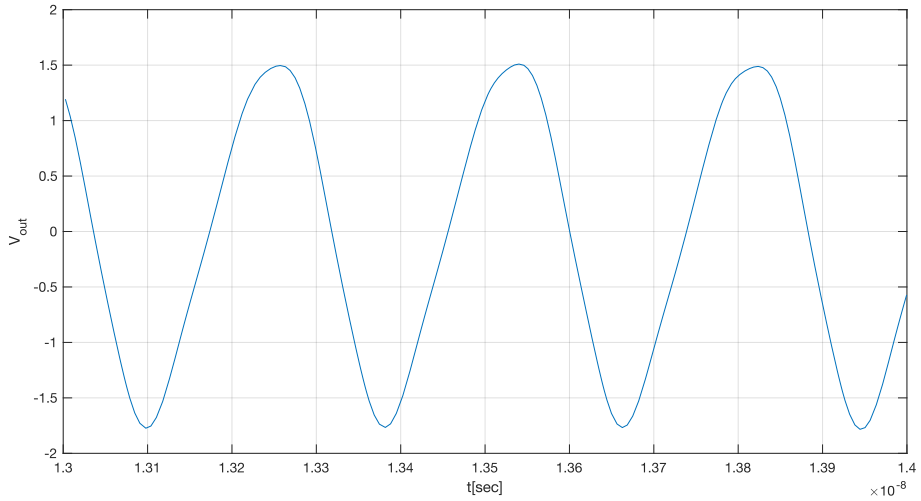
The design of the oscillator system (including the matching network) was carried out in Cadence Virtuoso using Spectre Simulation. Two types of simulations were performed

4.2.1 Transient Simulation

Transient simulation provides a time-domain analysis of the oscillator circuit. Its roles include:



(a) Transient Analysis of Oscillator



(b) Transient Analysis of Oscillator Zoomed

Figure 10: Transient Analysis

- **Time-Domain Analysis:** Displays how voltages and currents change over time, offering a detailed view of the circuit's dynamic behavior.
- **Startup Behavior:** Helps observe the startup behavior of the oscillator, ensuring it begins oscillating as expected.
- **Waveform Analysis:** Visualizes the actual waveforms of signals in the circuit, providing insights into their shape, amplitude, and frequency.
- **Nonlinear Effects:** Captures nonlinear effects and transient phenomena during the oscillator's operation.

4.2.2 Harmonic Balance Simulation

Harmonic balance simulation is a frequency-domain technique that analyzes steady-state oscillations. Its roles include:

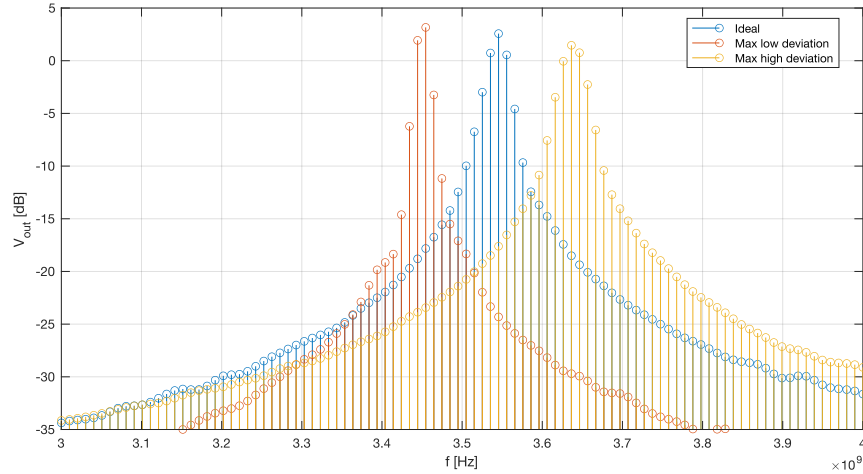


Figure 11: Harmonic of Oscillator+Matching Network

- **Frequency-Domain Analysis:** Provides information about the fundamental frequency and harmonics of the oscillator.
- **Steady-State Response:** Focuses on the steady-state response, making it ideal for analyzing periodic signals after transient effects have settled.
- **Spectral Content:** Studies the spectral content of the oscillator's output, including fundamental frequency and higher-order harmonics.
- **Component Variations:** We deal with manufacturer variations in the components used in our circuits as seen in (4). In order to have sufficient power transfer, operating frequency of the oscillator must be in the region where $S_{11} < -10[dB]$ for the antenna. Having HB simulations shows us this frequency and helps optimize the circuit to work properly with antenna.

4.3 Antenna

4.4 S-parameter (S11) Simulation

The S-parameter (S11) simulation for the antenna is crucial for several reasons:

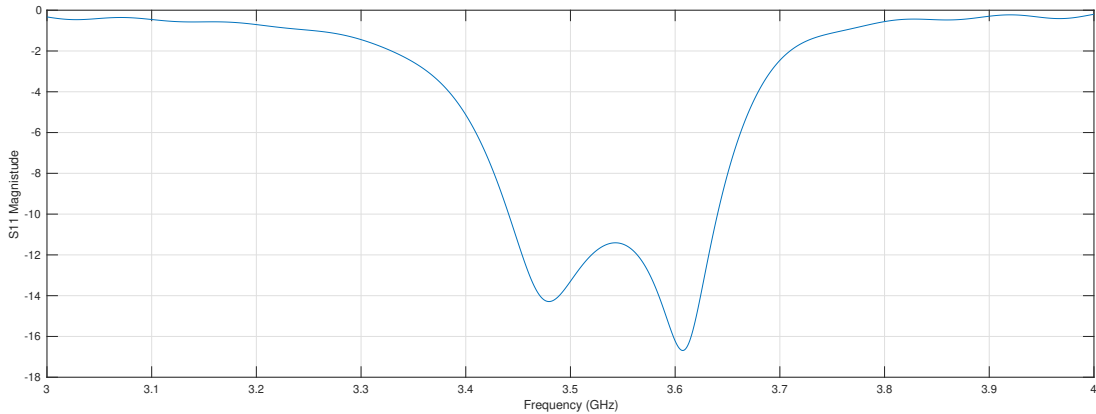


Figure 12: S11 of Wideband Patch Antenna

- **Reflection Coefficient:** It measures the amount of power reflected back from the antenna due to impedance mismatches.
- **Impedance Matching:** Helps optimize impedance matching to maximize power transfer efficiency.
- **Bandwidth:** Indicates the operating bandwidth of the antenna by showing frequency points where reflection is minimized or maximized.
- **Performance Verification:** Verifies the performance of the antenna design under various conditions, ensuring it meets specifications.

4.5 Far Field Simulation

The Far Field simulation⁹ provides critical insights into the antenna's radiation characteristics:

- **Radiation Pattern:** Shows how the antenna radiates electromagnetic waves in space, providing a visual representation of its directional characteristics.
- **Directivity:** Determines the directivity of the antenna, indicating the concentration of radiation in specific directions.
- **Gain:** Calculated from Far Field results, the gain assesses the antenna's performance in transmitting and receiving signals.
- **Beam Steering:** Analyzes the antenna's ability to steer beams in desired directions, essential for directive antennas.

Table 3: Far-Field Characteristics

Parameter	Value
Main Lobe Magnitude	6.22 dBi
Main Lobe Direction	0.0 deg
Angular Width at 3 dB	79.9 deg
Side Lobe Level	-15.6 dBi

⁹Polar plot of Far Field Gain can be found in Appendix

5 Analysis of Results

5.1 Matching Network

We now discuss the simulation output given in Fig 9

- **S_{11} (Input Reflection Coefficient):** Represents the reflected signal at the input port. Low values indicate good matching. The S_{11} plot shows a significant dip around 3.4 GHz, indicating excellent matching at this frequency. The low S_{11} value suggests effective impedance matching of the source to the network's input.
- **S_{12} (Reverse Transmission Coefficient):** Represents the reverse transmission from output to input. Low values indicate minimal reverse transmission. The S_{12} plot remains low across the frequency range, indicating minimal reverse transmission and good isolation.
- **S_{21} (Forward Transmission Coefficient):** Represents the transmitted signal from input to output. High values (close to 0 dB) indicate efficient transmission. The S_{21} plot peaks around 3.4 GHz, showing maximum forward transmission efficiency at this frequency. The gain is close to 0 dB, indicating nearly all input signal is transmitted to the output.
- **S_{22} (Output Reflection Coefficient):** Represents the reflected signal at the output port. Low values indicate good matching. The S_{22} plot shows a dip around 3.4 GHz, indicating good matching at the output port. The low reflection ensures that the 1k-ohm load is effectively matched.

The network is optimized for around 3.5[GHz], as shown by the dips in S_{11} and S_{22} and the peak in S_{21} . Outside this range, performance degrades, indicating the network is designed for narrow-band matching.

5.2 Oscillator

5.2.1 Transient Simulation

In plot Fig 10a, we see the transient waveform produced at the antenna. After carefully choosing the running I_{Q_1} and V_{DC} , we get a stable output on the load. Fig 10b showed the oscillations up close. We see no distortions and thus the oscillations produced are to our satisfaction.

5.2.2 Harmonic Balance Simulation

From Fig 11, we obtain operating frequencies to be in range 3.454[GHz] → 3.636[GHz]. This gives us an idea of how broad the bandwidth of the antenna must be.

5.2.3 Efficiency of Oscillator

The input power P_{DC} is calculated as the product of the supply voltage V_{CC} and the collector current I_C :

$$P_{DC} = V_{CC} I_C \quad (3)$$

The output power P_{ac} is given by the expression $\frac{V_{rms}^2}{R_L}$, where V_{rms} is the root mean square value of the output voltage, calculated as $\frac{V_{max}}{\sqrt{2}}$ for the output waveform:

$$P_{ac} = \frac{V_{rms}^2}{R_L} \quad (4)$$

The efficiency η is defined as the ratio of the output power P_{ac} to the input power P_{DC} :

$$\eta = \frac{P_{ac}}{P_{DC}} \quad (5)$$

For $V_{CC} = -V_{EE} = 8 [V]$ and a current mirror set to provide $3.36 [mA]$, we determine the peak voltage v_p to be $1.6 [V]$. This results in an efficiency η of approximately $20\%^{10}$

5.3 Antenna

5.3.1 S-parameter (S11) Simulation

In Fig 12, S_{11} parameters show a bandwidth of $3.441[GHz] \rightarrow 3.642[GHz]^{11}$. We see that we have a more than good enough dip at the interested frequencies, and all the possible operating frequencies of the oscillator come under the bandwidth ensuring high power transfer even in case of worst case deviations due to tolerances.

5.3.2 Far Field Simulation

The Far-Field results of the antenna, summarized in Table 3, indicate the following characteristics:

- **Main Lobe Magnitude:** 6.22 dBi, indicating the strength of the main radiation lobe.
- **Main Lobe Direction:** 0.0 deg, specifying the direction in which the main lobe is pointed.
- **Angular Width at 3 dB:** 79.9 deg, describing the angular coverage where the radiation is within 3 dB of the main lobe peak.
- **Side Lobe Level:** -15.6 dBi, showing the attenuation level of the side lobes compared to the main lobe.

These results are indicative of an antenna performance that meets or exceeds expectations, ensuring effective radiation characteristics suitable for its intended application.

5.4 Testing in Lab

The fabricated board was tested in the lab using a receiver and a Spectral Analyser. This was performed in the following stages.

5.4.1 Adding Ground to the PCB board

We realised that we should have added a ground pin to our PCB. In order to have a common ground, one of the via was extended as a ground terminal on a separate breadboard.

¹⁰noting that it has been shown by Krauss et al. (1980) that the maximum theoretical efficiency for this oscillator configuration is 25%, indicating that our efficiency is reasonably good

¹¹Bandwidth is defined as the region where $S_{11} < -10[dB]$

5.4.2 Testing the extended Circuit

The PCB was kept at a large enough distance from the receiver to test far field performance. The receiver was connected to a Spectral Analyzer using an RF Port.



(a) Ground Connection to the PCB

(b) Complete Test Setup

Figure 13: (a) Ground Connection to the PCB, and (b) Complete Test Setup

5.4.3 Obtained Spectrum

The obtained spectrum can be seen in Fig 14. We see that we have a spike at $3.6[GHz]$, which is within the design expectations.



Figure 14: Spectrum Analyzer connected to the receiver

6 Conclusion and Further Work

In summary, the design, simulation, and testing of the 3.5GHz Colpitts RF oscillator, along with the associated matching network and broadband antenna, successfully met the objectives set out at the beginning of this project. The oscillator design achieved excellent performance metrics, including high efficiency, minimal phase noise, and the generation of distortion-free signals at the target frequency of approximately 3.5GHz. By carefully selecting and tuning the components used in the PCB layout, we were able to minimize frequency deviations, ensuring that the oscillator consistently operated at or near the desired frequency.

The broadband antenna was designed to operate efficiently across a range of frequencies, accounting for potential variations due to component tolerances and manufacturing discrepancies. This flexibility in antenna performance is particularly crucial in real-world applications, where slight deviations in component values can impact overall system behavior. The successful integration of the oscillator, matching network, and antenna into a cohesive system underscores the robustness of the design approach and validates the theoretical models and simulations conducted throughout the project.

Despite these successes, there are several avenues for further exploration and enhancement. One potential area of future work involves pushing the limits of discrete-component RF circuit design to explore the feasibility of achieving even higher-order RF frequencies. This would involve addressing the physical constraints that arise with high-speed PCBs, such as parasitic inductance and capacitance, which become increasingly significant at higher frequencies. Understanding and mitigating these effects could lead to the development of oscillators capable of operating at frequencies well beyond 3.5GHz, thereby expanding the applicability of the design to a broader range of RF communication systems.

Another interesting direction for future research would be the exploration of differential oscillator topologies. Differential designs inherently offer greater stability and noise immunity compared to their single-ended counterparts. By expanding the current model to incorporate a differential configuration, we could potentially achieve larger signal swings, improved phase noise performance, and enhanced robustness against common-mode noise. This would not only improve the performance of the oscillator but also provide valuable learning opportunities in the realm of advanced RF design.

Additionally, integrating digitally tunable components, such as varactors, into the design could enable dynamic frequency control, allowing the oscillator to adapt to varying operational requirements in real-time. This capability would be particularly beneficial in systems that require frequency agility, such as cognitive radios and reconfigurable RF systems. Exploring the integration of non-discrete components, including those fabricated on integrated circuits (ICs), represents another promising direction for further development. By moving to an IC-based implementation, we could achieve even higher levels of integration, performance, and miniaturization, making the oscillator design more suitable for deployment in compact, high-performance RF modules. We can also switch to non-discrete components for the oscillator. In conclusion, while the current project has successfully demonstrated the feasibility and effectiveness of the 3.5GHz Colpitts oscillator design, there remains a wealth of opportunities for further research and development. By exploring these avenues, we can continue to advance the state of RF oscillator technology, contributing to the ongoing evolution of wireless communication systems.

7 Project Documentation

The project deliverables have been carefully documented and organized within a GitHub repository, structured according to the key tasks of the project. This final report provides an overview of the deliverables as they are presented in the repository.

The repository is divided into sections corresponding to each major task in the project:

- **Matching Network:** This section includes the LTSpice files and a Python script used for calculating component values.
- **Oscillator:** This section contains preliminary test files for the oscillator, created in both PSpice and LTSpice. The final design, which was used in the report, was implemented in Cadence Virtuoso and is accessible on the Micron Servers.
- **Antenna:** This section features CST projects for various antenna configurations considered during the design process. It also includes a folder named `Antenna-Calculator`, which contains Python scripts used to compute the antenna dimensions.
- **PCB Design:** This section includes the Altium files used for the PCB design.
- **MATLAB:** This section contains live scripts and .m files used for plotting the results.
- **Transistor:** This section contains the model of the BFP520/INF transistor.
- **Images:** This section includes schematics, results, and other visual content displayed in the `readme.md` file.

The documentation on GitHub serves as a comprehensive resource, detailing the project's development process and providing all necessary files and scripts to replicate or extend the work. This report focuses on summarizing the structure and content of the repository, ensuring clarity and accessibility for future reference.

8 Appendix

8.1 BFP520 Data

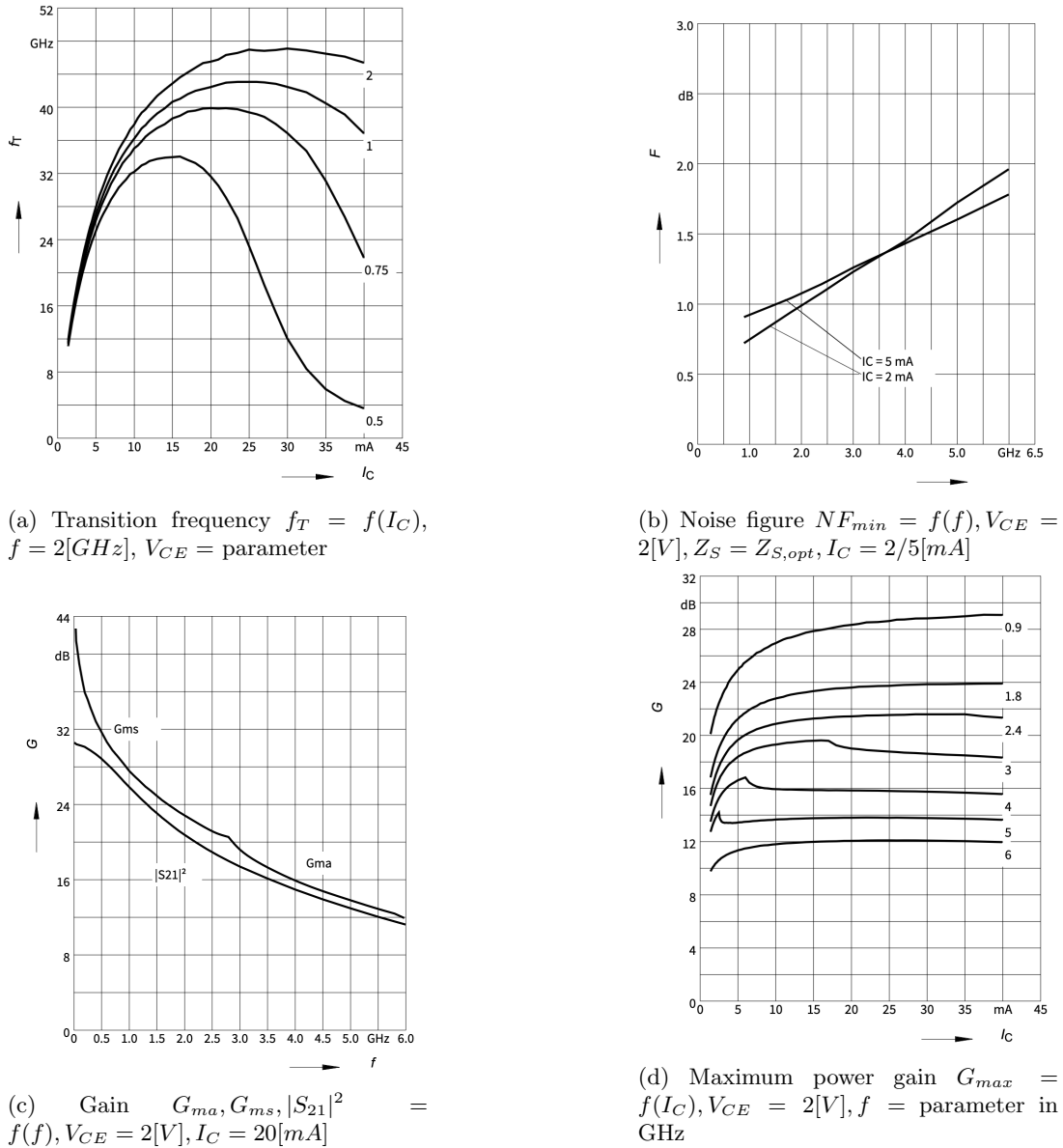


Figure 15: Combined plots of the BFP520's key characteristics.

8.2 Matching Network

8.2.1 Computation of L_s and C_s

We assume a central impedance Z_c such that $Z_c > \max(Z_s, Z_L)$, and then calculate the series and parallel reactive components on both sides.¹²

¹²In our case, all impedances are real

Source:

$$\begin{cases} Q_{src} = \sqrt{\frac{Z_c}{Z_s} - 1} \\ X_{src}^{parallel} = \frac{Z_c}{Q_{src}} \\ X_{src}^{series} = Q_{src} Z_s \end{cases} \quad (6)$$

Load:

$$\begin{cases} Q_{ld} = \sqrt{\frac{Z_c}{Z_L} - 1} \\ X_{ld}^{parallel} = \frac{Z_c}{Q_{ld}} \\ X_{ld}^{series} = Q_{ld} Z_L \end{cases} \quad (7)$$

$$L = \frac{X}{2\pi f_0} \quad \text{and} \quad C = \frac{1}{2\pi f_0 X} \quad (8)$$

for chosen X series/parallel

8.3 Oscillator

8.3.1 Mathematical Model of Feedback Oscillators

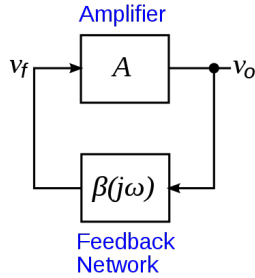


Figure 16: Block diagram of a feedback linear oscillator

A feedback oscillator circuit consists of two parts connected in a feedback loop: an amplifier A and an electronic filter $\beta(j\omega)$. The filter's purpose is to limit the frequencies that can pass through the loop so the circuit only oscillates at the desired frequency. Since the filter and wires in the circuit have resistance, they consume energy and the amplitude of the signal drops as it passes through the filter. The amplifier is needed to increase the amplitude of the signal to compensate for the energy lost in other parts of the circuit, so the loop will oscillate, as well as supply energy to the load attached to the output.

To determine the frequency (or frequencies) $\omega_0 = 2\pi f_0$ at which a feedback oscillator circuit will oscillate, the feedback loop is thought of as broken at some point to give an input and output port. A sine wave is applied to the input $v_i(t) = V_i e^{j\omega t}$ and the amplitude and phase of the sine wave after going through the loop $v_o = V_o e^{j(\omega t + \phi)}$ is calculated:

$$v_o = Av_f \quad \text{and} \quad v_f = \beta(j\omega)v_i \quad \text{so} \quad v_o = A\beta(j\omega)v_i$$

Since in the complete circuit v_o is connected to v_i , for oscillations to exist:

$$v_o(t) = v_i(t)$$

The ratio of output to input of the loop, $\frac{v_o}{v_i} = A\beta(j\omega)$, is called the loop gain. So the condition for oscillation is that the loop gain must be one:

$$A\beta(j\omega) = 1 \quad (9)$$

Since $A\beta(j\omega)$ is a complex number with two parts, a magnitude and an angle, the above equation actually consists of two conditions:

1. The magnitude of the gain (amplification) around the loop at ω_0 must be unity:

$$|A\beta(j\omega)| = 1 \quad (10)$$

so that after a trip around the loop the sine wave is the same amplitude. If the loop gain were greater than one, the amplitude of the sinusoidal signal would increase as it travels around the loop, resulting in a sine wave that grows exponentially with time, without bound. If the loop gain were less than one, the signal would decrease around the loop, resulting in an exponentially decaying sine wave that decreases to zero.

2. The sine wave at the end of the loop must be in phase with the wave at the beginning of the loop. Since the sine wave is periodic and repeats every 2π radians, this means that the phase shift around the loop at the oscillation frequency ω_0 must be zero or a multiple of 2π radians (360°):

$$\angle A + \angle \beta = 2n\pi \quad \text{where } n \in \{0, 1, 2, \dots\} \quad (11)$$

Equations (10) and (11) are called the Barkhausen stability criterion. It is a necessary but not a sufficient criterion for oscillation. An equivalent condition often used instead of the Barkhausen condition is that the circuit's closed loop transfer function (the circuit's complex impedance at its output) have a pair of poles on the imaginary axis.

8.3.2 Operating Frequency and Startup Condition for Coll-pits Oscillator

We analyse the small signal model of Fig 2 and derive the operating frequency and the startup conditions for reliable functioning of the oscillator. [5]

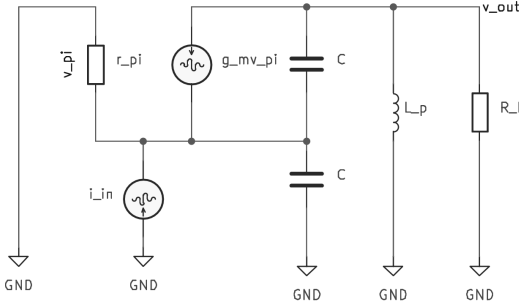


Figure 17: Small Signal Model for Collpits Oscillator

We have the following equations:

$$i_{in} = -\frac{v_{\pi}}{r_{\pi}} - sC(v_{out} + 2v_{\pi}) \quad (12)$$

$$0 = g_m v_{\pi} + sC(v_{out} + v_{\pi}) + \frac{v_{out}}{sL_p} + \frac{v_{out}}{R_L} \quad (13)$$

Solving (13), the frequency response comes out to be

$$\frac{v_{out}}{i_{in}} = \frac{r_{\pi}L_pR_L(s^2C + sg_m)}{r_{\pi}C^2L_pR_Ls^3 + (-r_{\pi}CL_pR_Lg_m + 2r_{\pi}CL_p + CL_pR_L)s^2 + (2r_{\pi}CR_L + L_p)s + R_L} \quad (3)$$

Put $s = j\omega$ and let Im of denominator $\rightarrow 0$

$$\omega_0 = \sqrt{\frac{2r_\pi CR_L + L_p}{r_\pi C^2 L_p R_L}} \quad (14)$$

Assuming $r_\pi \rightarrow \infty$, as is the case in MOS, we reach the well-known expression $\omega_0 = \sqrt{\frac{1}{L \frac{C+C}{C+C}}}$
For sustained oscillations, we need

$$-(-r_\pi CL_p R_L g_m + 2r_\pi CL_p + CL_p R_L) \omega_0^2 + R_L > 0 \quad (15)$$

This gives us

$$R_L g_m - \frac{R_L}{r_\pi} - 2 > 0 \quad (16)$$

Thus, we need to set R_L ¹³ accordingly at the oscillating frequency, giving us a lower bound for load and thus a need for a matching network [3]

8.4 Transmission Line Formulas

8.4.1 Parameters of a Microstrip line for required Z_0

The purpose of the following theory is to fix the input impedance of the patch antenna using a microstrip line.

For $\frac{W}{d} \geq 1$, we have

$$Z_0 = \frac{120\pi}{\sqrt{\epsilon_{eff}}} \frac{1}{\sqrt{\frac{W}{d} + 1.393 + 0.667 \ln\left(\frac{W}{d} + 1.444\right)}} \quad (17)$$

Solution:

For $W/d < 2$

$$\frac{W}{d} = \frac{8e^A}{e^{2A} - 2} \quad (18)$$

For $W/d > 2$

$$\frac{W}{d} = \frac{2}{\pi} \left[B - 1 - \ln(2B - 1) + \frac{\epsilon_r - 1}{2\epsilon_r} \left(\ln(B - 1) + 0.39 - \frac{0.61}{\epsilon_r} \right) \right] \quad (19)$$

where

$$A = \frac{Z_0}{60} \sqrt{\frac{\epsilon_r + 1}{2}} + \frac{\epsilon_r - 1}{\epsilon_r + 1} \left(0.23 + \frac{0.11}{\epsilon_r} \right) \quad (20)$$

and

$$B = \frac{377\pi}{2Z_0 \sqrt{\epsilon_r}} \quad (21)$$

¹³This is similar to the condition found in Razavi for NMOS

8.4.2 Patch Antenna Dimensions

We measure the width and ϵ_{eff} of the patch using

$$W = \frac{1}{2f_0\sqrt{\mu_0\epsilon_0}} \sqrt{\frac{2}{\epsilon_r + 1}} \quad (22)$$

$$\epsilon_{eff} = \frac{\epsilon_r + 1}{2} + \frac{\epsilon_r - 1}{\sqrt{1 + \frac{12h}{W}}} \quad (23)$$

Then, the length is measured as

$$\frac{\Delta L}{h} = 0.412 \frac{(\epsilon_{eff} + 0.3) \left(\frac{W}{h} + 0.264 \right)}{(\epsilon_{eff} - 0.258) \left(\frac{W}{h} + 0.8 \right)} \quad (24)$$

$$L_{eff} = \frac{c}{2f_0\sqrt{\epsilon_{eff}}} \quad (25)$$

and

$$L = L_{eff} - 2\Delta L \quad (26)$$

8.4.3 Constraints on the dimensions of the ground plane

Enough spacing must be given to the antenna edges to avoid fringing effects, thus inducing a minimum size for the ground plane and PCB

$$\begin{cases} \lambda_{eff} = \frac{c}{f_0} \sqrt{\epsilon_{eff}} \\ L_{gnd} \geq L + 2 \times \frac{\lambda_{eff}}{4} \\ W_{gnd} \geq W + 2 \times \frac{\lambda_{eff}}{4} \end{cases} \quad (27)$$

8.5 Antenna

8.5.1 Far-Field Simulation Output

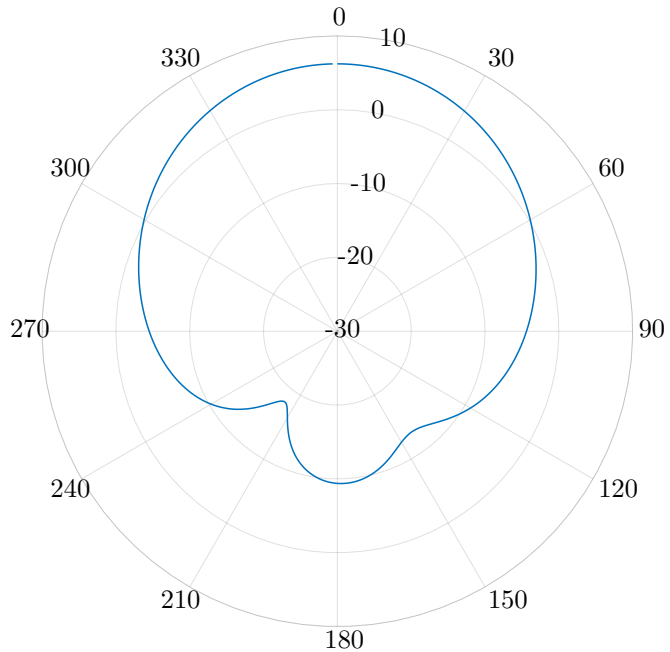


Figure 18: Far-Field of Wideband Patch Antenna

8.6 Layout

8.6.1 Table of Components

Table 4: Used Components and Tolerances

Part Number	Value	Tolerance
LQG15HN2N0B02D	2nH	0.1nH
LQP03TN2N0B02D	2nH	0.1nH
LQG15WZ10NG02D	10nH	0.2nH
EEU-FC1V102SB	1000uF	200uF
GRM1555C1H3R4WA01D	3.4pF	0.05pF
04023J0R2PBSTR Kyocera AVX	0.2pF	0.02pF

8.6.2 PCB Schematic

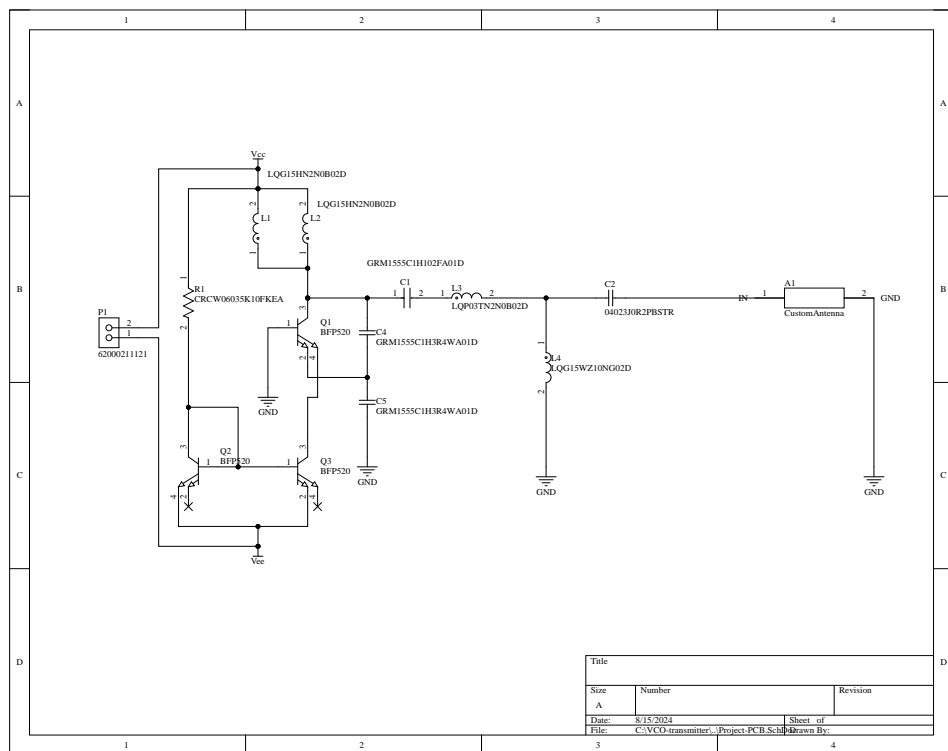


Figure 19: Oscillator+Matching Network Schematic

References

- [1] Ahmed Alsager. Design and analysis of microstrip patch antenna arrays. 05 2011.
- [2] Macera Giuseppe. *Comparison of Voltage-Controlled-Oscillator Architectures for Implementation in 180 nm SiGe Technology*. PhD thesis, 12 2016.
- [3] Timothy K. Johnson. A colpitts oscillator design technique using s-parameters. 1986.
- [4] Xiaoyong Li, Sudip Shekhar, and David Allstot. G/sub m/-boosted common-gate lna and differential colpitts vco/qvco in 0.18-/spl mu/m cmos. *Solid-State Circuits, IEEE Journal of*, 40:2609 – 2619, 01 2006.
- [5] David M Pozar. *Microwave engineering; 3rd ed.* Wiley, Hoboken, NJ, 2005.
- [6] Behzad Razavi. *Design of Analog CMOS Integrated Circuits*. McGraw-Hill, first edition, 2001.
- [7] Jin-Dong Zhang, Lei Zhu, Qiong-Sen Wu, Neng-Wu Liu, and Wen Wu. A compact microstrip-fed patch antenna with enhanced bandwidth and harmonic suppression. *IEEE Transactions on Antennas and Propagation*, 64(12):5030–5037, 2016.